Supplementary materials for "Quantum engineering of radiative properties of molecules inside a nanoscale mesoscopic system"

Ilya V. Doronin,[1,2] Alexander A. Zyablovsky,[1,3,4] Evgeny S. Andrianov,[1,3] Alexey S. Kalmykov,[2] Anton S. Gritchenko,[2] Boris N. Khlebtsov,[5] Shao-Peng Wang,[6] Bin Kang,[6] Victor I. Balykin,[2] Pavel N. Melentiev,[2,7,*]

[1]Moscow Institute of Physics and Technology, Institutskiy per. 9, Moscow, 141700, Russia

[2]Institute of Spectroscopy of Russian Academy of Sciences, Fizicheskaya str. 5, Troitsk, Moscow, 108840, Russia

[3]Institute for Theoretical and Applied Electromagnetics, Izhorskaya str. 13, Moscow, 125412, Russia

[4]Kotelnikov Institute of Radioengineering and Electronics RAS, Mokhovaya str. 11-7, Moscow, 125009, Russia

[5]Institute of Biochemistry and Physiology of Plants and Microorganisms, Saratov Scientific Centre of the Russian Academy of Sciences, Prospekt Entuziastov 13, Saratov, 410049, Russia

[6]State Key Laboratory of Analytical Chemistry for Life Science and Collaborative Innovation Center of Chemistry for Life Sciences, School of Chemistry and Chemical Engineering, Nanjing University, 163 Xianlin Road, Nanjing, 210023, P. R. China

[7]Higher School of Economics, National Research University, Myasnitskaya str. 20, Moscow, 101000, Russia

*Corresponding author's email: melentiev@isan.troitsk.ru

Section 1 *Fluorescence of Cy-7.5 dye in dielectric core-shell nanoparticle*

In this section, we describe our model for studying the effect of fluorescence quenching of the Cy-7.5 dye in polydopamine in more detail compared to the main text (Section 3.1, see also Fig. 1a). We consider two energy levels of a single dye molecule, the ground state, $|G_{dye}\rangle$, and the excited singlet state, $|E_{dye}\rangle$, with transition frequency ω_0 (for simplicity, we assume that the frequencies of all dye molecules are the same). The transition between these levels leads to fluorescence. We assume that the PDA shell has a number of states $|E^i_{PDA}\rangle$. The PDA shell interacts with the dye molecule $|E_{dye}\rangle$ via Foerster energy transfer, which leads to non-radiative transitions between the excited states of the dye molecules and the set of states in the PDA shell (see Fig. 1a in the main text). This interaction is responsible for fluorescence quenching.[1] For simplicity, we assume that the pump rate in the system is much slower than the decay rate of the states $|E_{dye}\rangle$ and $|E^i_{PDA}\rangle$ (estimates can be found in Section 3 of Supplementary Materials). Therefore, the states corresponding to the simultaneous excitation of the PDA and Cy-7.5 dye levels are hardly populated and can be neglected. For this reason, we consider only three states of the core-shell dielectric nanoparticle system: $|E\rangle = |E_{dye}\rangle \otimes |G^1_{PDA}\rangle \otimes ...$ (the dye molecule is excited),

$|PDA_i\rangle = |G_{dye}\rangle \otimes |E^i_{PDA}\rangle \otimes |G^1_{PDA}\rangle \otimes |G^2_{PDA}\rangle \otimes ...$ (one of the PDA states is excited), $|G\rangle = |G_{dye}\rangle \otimes |G^1_{PDA}\rangle \otimes ...$ (the ground state).

The considered system can be described by the Hamiltonian:

$$\hat{H}_1 = \hbar\omega_0 \hat{\sigma}^\dagger \hat{\sigma} + \sum_i \hbar\omega^i_{PDA} \hat{s}^\dagger_i \hat{s}_i \qquad \text{(S1)}$$

where $\hat{\sigma}^\dagger = |E\rangle\langle G|$ and $\hat{\sigma} = |G\rangle\langle E|$ are raising and lowering operators of the dye molecule and obey the anticommutation relation $\{\hat{\sigma}^\dagger; \hat{\sigma}\} = 1$; $\hat{s}^\dagger_i = |PDA_i\rangle\langle G|$ and $\hat{s}_i = |G\rangle\langle PDA_i|$ are raising and lowering operators of PDA states and obey the anticommutation relation $\{\hat{s}^\dagger_i; \hat{s}_i\} = 1$; $\hbar\omega^i_{PDA}$ are energies of PDA states.

To describe the transition between system states, one must consider the interaction of the system with the environment. In the general case, the Hamiltonian of a system interacting with its environment can be written as

$$\hat{H} = \hat{H}_S + \hat{H}_R + \hat{H}_{SR}, \qquad \text{(S2)}$$

The first term in (2) is the Hamiltonian of the isolated system. The second term in (2) is composed of the Hamiltonians of four separate reservoirs:

$$\hat{H}_R = \hat{H}^{rad}_R + \hat{H}^{n}_R + \hat{H}^{deph}_R + \hat{H}^{pump}_R + \hat{H}^{PDA}_R \qquad \text{(S3)}$$

The first term in Equation S3 is the Hamiltonian of the EM field modes of free space, $\hat{H}^{rad}_R = \sum_{\mathbf{k},\lambda} \hbar\omega_{\mathbf{k}} \hat{c}^\dagger_{\mathbf{k},\lambda} \hat{c}_{\mathbf{k},\lambda}$. The operators $\hat{c}_{\mathbf{k},\lambda}$ and $\hat{c}^\dagger_{\mathbf{k},\lambda}$ are the annihilation and creation operators of a photon in the mode of the EM field with frequency $\omega_{\mathbf{k}}$, wave vector $\mathbf{k}$ and polarization λ. The Hamiltonian of the interaction of this reservoir with the system has the form [2-3]

$$\hat{H}^{rad}_{SR} = \sum_{\mathbf{k},\lambda} \hbar\kappa^{rad}_{\mathbf{k},\lambda} \hat{\sigma}^\dagger \hat{c}_{\mathbf{k},\lambda} + h.c., \qquad \text{(S4)}$$

where $\kappa^{rad}_{\mathbf{k},\lambda} = -\mathbf{d}_{dye}\mathbf{E}_{\mathbf{k},\lambda}(\mathbf{r}_{dye})/\hbar$ is the interaction constant; $\mathbf{d}_{dye}$ is the matrix element of dipole transition from the excited state of the dye to the ground state; $\mathbf{E}_{\mathbf{k},\lambda}(\mathbf{r}_{dye})$ is the electric; d_{dye} can be estimated by the radiation decay rate γ_{rad} of the dye molecules as follows [4] $d_{dye} = \sqrt{\frac{3\gamma_{rad}\hbar c^3}{4\omega_0^3}}$.

The second term in (3) is the Hamiltonian of the optical phonons in the active medium, which is responsible for the nonradiative decay $\hat{H}^n_R = \sum_{\mathbf{k},\lambda} \hbar\omega_{\mathbf{k}} \hat{f}^\dagger_{\mathbf{k},\lambda} \hat{f}_{\mathbf{k},\lambda}$. The operators $\hat{f}_{\mathbf{k},\lambda}$ and $\hat{f}^\dagger_{\mathbf{k},\lambda}$ are annihilation and creation operators of a phonon with frequency $\omega_{\mathbf{k}}$, wave vector $\mathbf{k}$ and polarization λ. The Hamiltonian of the interaction of this reservoir with the system has the form [2-3]

$$\hat{H}^n_{SR} = \sum_{\mathbf{k},\lambda} \hbar\kappa^n_{\mathbf{k},\lambda} \hat{\sigma}^\dagger \hat{f}_{\mathbf{k},\lambda} + h.c., \qquad \text{(S5)}$$

where $\kappa^n_{\mathbf{k},\lambda}$ is interaction constant.

The third term in the Equation S3 is the Hamiltonian of the vibrational degrees of freedom of the PDA shell, $\hat{H}_R^{deph} = \sum_j \hbar\omega_j \hat{b}_j^\dagger \hat{b}_j$. The operators $\hat{b}_j$, $\hat{b}_j^\dagger$ are annihilation and creation operators of the oscillations in the PDA shell with the frequency ω_j. The following Hamiltonian describes the interaction of the reservoir with the system [2-3]

$$\hat{H}_{SR}^{deph} = \sum_j \hbar(\hat{b}_j^\dagger + \hat{b}_j) \sum_{k,n} \kappa_j^{deph} |k\rangle\langle n| + h.c., \tag{S6}$$

where $|k\rangle$ and $|n\rangle$ are either $|E\rangle$ or $|PDA_i\rangle$. κ_j^{deph} are the interaction constants.

The fourth term in (S3) represents pumping reservoir which can be effectively described by the Hamiltonian $\hat{H}_R^{pump} = \sum_j \hbar\omega_j \hat{p}_j^\dagger \hat{p}_j$, i.e. reservoir of two-level systems with transition frequencies ω_j and positive population inversion. This reservoir describes the incoherent pumping of the system. $\hat{p}_j$ and $\hat{p}_j^\dagger$ are transition operators to the ground state and the excited state of *j*-th two-level system, respectively. The pumping reservoir interacts with the electronic degrees of freedom of the molecule as: [2-3]

$$\hat{H}_{SR}^{pump} = \sum_j \hbar\kappa_j^{pump} \hat{\sigma}^\dagger \hat{p}_j + h.c. \tag{S7}$$

with the interaction constant κ_j^{pump}.

The fifth term in (S3) represents optical phonons in PDA and can be effectively described by the Hamiltonian $\hat{H}_R^{PDA} = \sum_j \hbar\omega_j \hat{q}_j^\dagger \hat{q}_j$, i.e. reservoir of two-level systems with transition frequencies ω_j. This reservoir describes the non-radiative decay of PDA states. $\hat{q}_j$ and $\hat{q}_j^\dagger$ are transition operators to the ground state and the excited state of *j*-th two-level system, respectively. Hamiltonian of the interaction of this reservoir with the system has the form:

$$\hat{H}_{SR}^{PDA} = \sum_j \sum_i \hbar\kappa_j^{PDA} \hat{s}_i^\dagger \hat{q}_j + h.c. \tag{S8}$$

with the interaction constant κ_j^{PDA}.

Now we use the Born-Markov approximation to exclude reservoir variables and obtain the Lindblad equation for the system's density matrix: [5]

$$\frac{\partial\hat{\rho}}{\partial t} = -\frac{i}{\hbar}\left[\hat{H}_S, \hat{\rho}\right] + \hat{L}_{rad}(\hat{\rho}) + \hat{L}_n(\hat{\rho}) + \hat{L}_{PDA}(\hat{\rho}) + \hat{L}_{deph}(\hat{\rho}) + \hat{L}_{pump}(\hat{\rho}) \tag{S9}$$

$\hat{L}_i(\hat{\rho})$ are the Lindblad superoperators having the form

$$\hat{L}_{rad}(\hat{\rho}) = \frac{\gamma_{rad}}{2}\left(2\hat{\sigma}\hat{\rho}\hat{\sigma}^\dagger - \hat{\sigma}^\dagger\hat{\sigma}\hat{\rho} - \hat{\rho}\hat{\sigma}^\dagger\hat{\sigma}\right)$$

$$\hat{L}_n(\hat{\rho}) = \frac{\gamma_n}{2}\left(2\hat{\sigma}\hat{\rho}\hat{\sigma}^\dagger - \hat{\sigma}^\dagger\hat{\sigma}\hat{\rho} - \hat{\rho}\hat{\sigma}^\dagger\hat{\sigma}\right)$$

$$\hat{L}_{PDA}(\hat{\rho}) = \frac{\tilde{\gamma}_n}{2}\sum_i\left(2\hat{s}_i\hat{\rho}\hat{s}_i^\dagger - \hat{s}_i^\dagger\hat{s}_i\hat{\rho} - \hat{\rho}\hat{s}_i^\dagger\hat{s}_i\right)$$

$$\hat{L}_{deph}(\hat{\rho}) = \sum_{i,j} \frac{\gamma_{ph}}{2N_{PDA}} \left(2\hat{S}_i^\dagger \hat{S}_j \hat{\rho} \hat{S}_j^\dagger \hat{S}_i - \hat{S}_j^\dagger \hat{S}_i \hat{S}_i^\dagger \hat{S}_j \hat{\rho} - \hat{\rho} \hat{S}_j^\dagger \hat{S}_i \hat{S}_i^\dagger \hat{S}_j \right)$$

$\hat{S}_i$ is one of operators $\hat{s}_k$, or $\hat{\sigma}$; N_{PDA} is the effective number of PDA states.

$$\hat{L}_{pump}(\hat{\rho}) = \frac{\gamma_{pump}}{2} \left(2\hat{\sigma}^\dagger \hat{\rho} \hat{\sigma} - \hat{\sigma} \hat{\sigma}^\dagger \hat{\rho} - \hat{\rho} \hat{\sigma} \hat{\sigma}^\dagger \right).$$

$\hat{L}_{rad}(\hat{\rho})$ describes radiative decay of Cy-7.5 dye population inversion; $\hat{L}_n(\hat{\rho})$ describes nonradiative decay of Cy-7.5 dye population inversion; $\hat{L}_{PDA}(\hat{\rho})$ describes nonradiative decay of PDA states; $\hat{L}_{deph}(\hat{\rho})$ describes dephasing of dye molecules polarization within PDA; $\hat{L}_{pump}(\hat{\rho})$ describes the incoherent pumping of the dye molecules. The rates γ_i^{nm} included in the Lindblad superoperators are determined according to the Fermi's golden rule $\gamma_i^{nm} = G(\Delta\omega) \left| \langle n | \hat{H}_{SR}^i | m \rangle \right|^2$, for transitions from a state $|n\rangle$ to a state $|m\rangle$,[6] and obey the Kubo-Martin-Schwinger condition $\gamma_i^{nm} / \gamma_i^{mn} = \exp[-(E_n - E_m)/kT_i]$, [4, 7-8] where E_n is the energy of *n*-th eigenstate, and T_i is the temperature of the reservoir *i*.

To summarize this section, let us describe all possible transitions between system states. First class of transitions is the relaxation of the population inversion of the dye molecules, which includes both radiative and nonradiative transitions. This process leads to the transition from the excited states of the dye molecule to the ground state, $|E\rangle \to |G\rangle$. Second class is the relaxation of the population inversion of the PDA states via non-radiative transitions. This process leads to the transition from the PDA states to the ground state, $|PDA_i\rangle \to |G\rangle$. The dephasing processes in the dye molecules lead to the destruction of the polarizations phases in the dye molecules and cause third class of transitions between excited states of the dye molecule, $|E\rangle$, and PDA states, $|PDA_i\rangle$. This process determines the linewidth of a dye molecule in polydopamine. Finally, the optical pumping of the system leads to the fourth class of transitions, $|G\rangle \to |E\rangle$. All transitions are schematically shown in Fig. 1a in the main text.

From the master Equation S9, kinetic equations can be derived for the occupation of the excited state of the dye molecules, $n_E = \mathrm{Tr}\left(\hat{\rho}(t)\hat{\sigma}^\dagger\hat{\sigma}\right)$, the occupation of the ground state of the dye molecules, $n_G = \mathrm{Tr}\left(\hat{\rho}(t)\hat{\sigma}\hat{\sigma}^\dagger\right)$, and the total occupation of the PDA states, $n_{PDA} = \mathrm{Tr}\left(\hat{\rho}(t)\sum_i \hat{s}_i^\dagger \hat{s}_i\right)$. The resulting equations have the form

$$\dot{n}_E = -(\gamma_{rad} + \gamma_n) n_E + \gamma_{pump} n_G - \gamma_{ph} n_E + \tilde{\gamma}_{ph} n_{PDA}$$

$$\dot{n}_{PDA} = \gamma_{ph} n_E - \tilde{\gamma}_{ph} n_{PDA} - \tilde{\gamma}_n n_{PDA} \qquad \text{(S10)}$$

$$\dot{n}_G = (\gamma_{rad} + \gamma_n) n_E - \gamma_{pump} n_G + \tilde{\gamma}_n n_{PDA}$$

Here γ_{rad} is the radiative decay rate of Cy-7.5 dye population inversion; γ_n is the non-radiative decay rate of Cy-7.5 dye population inversion; γ_{pump} is the incoherent pump rate; γ_{ph} is the dephasing rate responsible for the natural spectral width of Cy-7.5 within PDA; $\tilde{\gamma}_{ph}$ is the rate of inverse transition (from PDA states to the excited Cy-7.5 singlet state); $\tilde{\gamma}_n$ is the non-radiative decay rate of PDA states.

The final step is to determine the rates in Equation S10 from experimental data. First, the sum of the radiative and nonradiative decay rates equals the fluorescence decay rate determined by the experiment (see Fig. 2b in the main text). The radiative decay rate can be calculated as the quantum yield of the Cy-7.5 dye multiplied by the total fluorescence decay rate. The quantum yield of the Cy-7.5 dye is known to be 0.1.[9] Second, the dephasing rate γ_{ph} can be estimated from the linewidth of Cy-7.5 dye emission. The effective number of PDA states N_{PDA} need not be determined because this this value disappears from the final equations. However, Equation S10 contains not only the rate γ_{ph}, but also the inverse rate $\tilde{\gamma}_{ph}$ describing the probability flux from $|PDA_i\rangle$ states to $|E\rangle$. This rate can be estimated as $\gamma_{ph}\exp[-\hbar(\omega_0-\langle\omega_{PDA}\rangle)/kT]/N_{PDA}$, where $\langle\omega_{PDA}\rangle$ is the effective frequency of PDA levels interacting with the excited state. We use the factor $\exp[-\hbar(\omega_0-\langle\omega_{PDA}\rangle)/kT]/N_{PDA}$ as an optimization parameter in our calculations to obtain the best fit of the experimental data for the fluorescence cross section of both the dielectric nanoparticle and the plasmonic nanoparticle simultaneously. Finally, the pump rate γ_{pump} is estimated from the intensity of the pump laser used (see details in Section 3 of supplementary materials).

Section 2 ***Fluorescence of Cy-7.5 in plasmonic Core-Shell nanoparticle***

In this section, we consider our model of fluorescence of Cy-7.5 molecules and the suppression of quenching in PDA by optical coupling to a plasmonic nanoparticle in more detail (Fig. 1b in the main text). To describe Cy-7.5 molecules located in the PDA shell coupled to a plasmonic nanoparticle, we need to consider the following subsystems. First, a plasmonic mode with equidistant energy states $|n\rangle, n=0,1...$. Second, N dye molecules located in the hotspot of the plasmonic mode, with ground states $|G_j\rangle$ and excited singlet states $|E_j\rangle$ with transition frequency ω_0 (for simplicity, we assume that the frequencies of all dye molecules are the same). Finally, a set of PDA states is denoted as $|E^i_{PDA}\rangle$. Note that, unlike in Section 1 in supplementary materials, we consider the collective states of N dye molecules. The reason is that the plasmonic nanorod couples to the collective state of dye molecules, not to a single molecule. [10-11] Similar to Section 1 in supplementary materials, we assume that the average number of excitations in the system is less than one (see Section 3 in Supplementary materials). Therefore, the ground state (without excitations in any of the subsystems) and states with a single excitation are sufficient to describe the dynamics. These states are explicitly listed in the remainder of this section.

A gold nanoparticle in the form of a spheroid supports two dipole resonances. Using[12-13] equations 7.9-7.10 (see also Fig. 12.5 in Ref.[14]), we obtain that these resonances occur at two different frequencies, namely at $\lambda = 500nm$ and $\lambda = 834nm$. Note that the PDA with which the gold particle is coated has a dielectric permittivity of 2.2.[15-16]Therefore, we only consider a plasmonic mode at

$\lambda = 834nm$ that is close to Cy-7.5 transition frequency and the frequency of the external driving field. Following the second quantization procedure[5], the Hamiltonian of the electric field of the plasmonic nanoparticle takes the form of the Hamiltonian of a harmonic oscillator, $\hat{H}_p = \hbar\omega_p \hat{a}^\dagger \hat{a}$, where creation and annihilation operator, $\hat{a}^\dagger$ and $\hat{a}$, obey boson commutation relation $\left[\hat{a}, \hat{a}^\dagger\right] = \hat{1}$. The plasmon electric field has the form $\hat{\mathbf{E}}_p = \mathbf{E}_p^{(0)}(\mathbf{r})\left(\hat{a} + \hat{a}^\dagger\right)$. The magnitude $\mathbf{E}_p^{(0)}(\mathbf{r})$ has the meaning of the electric field "per one plasmon" and is determined by the normalization condition $\frac{1}{8\pi}\int_V d^3\mathbf{r} \left.\frac{\partial\left(\omega \operatorname{Re}\varepsilon(\mathbf{r},\omega)\right)}{\omega}\right|_{\omega_p} \left|\mathbf{E}_p^0(\mathbf{r})\right|^2 = \hbar\omega_p$.

We assume that there is a dipole transition between the respective excited states $\left|E_j\right\rangle$ and ground states $\left|G_j\right\rangle$ of the dye molecules with matrix element $\mathbf{d}_{dye}^{(j)}$ that is the dipole moment operator of the *j*-th molecule is $\hat{\mathbf{d}}_{dye}^{(j)} = \mathbf{d}_{dye}^{(j)}\left(\left|E_j\right\rangle\left\langle G_j\right| + \left|G_j\right\rangle\left\langle E_j\right|\right)$. The operators $\left|E_j\right\rangle\left\langle G_j\right|$ and $\left|G_j\right\rangle\left\langle E_j\right|$ describe transitions from state $\left|G_j\right\rangle$ to state $\left|E_j\right\rangle$ and vice versa. In the dipole approximation, the Hamiltonian of the interaction of a plasmonic nanoparticle with dye molecules has the form $\hat{H}_{\text{int}} = \sum_{j=1}^{N} -\hat{\mathbf{d}}_{dye}^{(j)}\hat{\mathbf{E}}_p\left(\mathbf{r}_j\right)$, where $\mathbf{r}_j$ is the radius vector of the position of *j*-th molecule.

Summarizing the above, we obtain the following Hamiltonian of the system:

$$\hat{H}_{dye-plasmon} + \hat{H}_{PDA}, \tag{S11}$$

where $\hat{H}_{dye-plasmon} = \hbar\omega_0 \sum_j \hat{\sigma}_j^\dagger \hat{\sigma}_j + \hbar\omega_p \hat{a}^\dagger \hat{a} + \hbar\Omega_R \sum_j (\hat{a}\hat{\sigma}_j^\dagger + \hat{a}^\dagger \hat{\sigma}_j)$ and $\hat{H}_{PDA} = \sum_i \hbar\omega_{PDA}^i \hat{s}_i^\dagger \hat{s}_i$. $\hat{\sigma}_j^\dagger = \left|E_j\right\rangle\left\langle G_j\right|$ and $\hat{\sigma}_j = \left|G_j\right\rangle\left\langle E_j\right|$ are the raising and lowering operators of *j*-th dye molecule obeying the anticommutator relation $\left\{\hat{\sigma}_j^\dagger; \hat{\sigma}_j\right\} = 1$; $\hat{s}_i^\dagger$ and $\hat{s}_i$ are raising and lowering operators of the PDA states (see Section 1 in Supplementary materials); $\Omega = -\mathbf{d}_{dye}^{(j)}\mathbf{E}_p^{(0)}\left(\mathbf{r}_j\right)/\hbar$ is the Rabi constant of the interaction between *j*-th molecule and plasmon mode. For simplicity, we assume that the Rabi constant is the same for all dye molecules.

The Hamiltonian in Equation S11 has the set of operators, $\hat{s}_i^\dagger$ and $\hat{s}_i$, which are included in $\hat{H}_{PDA}$ only. Therefore, the problem of finding eigenstates of Hamiltonian in Equation S11 reduces to finding states of $\hat{H}_{dye-plasmon}$ and $\hat{H}_{PDA}$. $\hat{H}_{dye-plasmon}$ is the Tavis-Cummings Hamiltonian and its eigenstates can be found exactly.[10-11] Since we are working in low excitation approximation, we only need to find the ground state and the set of eigenstates with one excitation. The ground state $\left|G\right\rangle$ of the system is composed of the ground state of the Tavis-Cummings model $\left|0\right\rangle \otimes \left|G_1\right\rangle \otimes ... \otimes \left|G_N\right\rangle$ and the ground state of the PDA levels, so that $\left|G\right\rangle = \left|0\right\rangle \otimes \left|G_1\right\rangle \otimes ... \otimes \left|G_N\right\rangle \otimes \left|G_{PDA}^1\right\rangle \otimes ...$. Eigenstates with one excitation are:[10-11, 17]

- *N*-1 dark states with transition frequency $\omega_D = \omega_0$ arising from Tavis-Cummings model

- the PDA states $\left|0\right\rangle \otimes \left|G_1\right\rangle \otimes ... \otimes \left|G_N\right\rangle \otimes \left|E_{PDA}^i\right\rangle \otimes \left|G_{PDA}^1\right\rangle \otimes ...$

- lower polariton state with transition frequency $\omega_{LP} = \frac{\omega_0 + \omega_p}{2} - \sqrt{\frac{(\omega_0 - \omega_p)^2}{4} + \Omega^2 N}$ and wavefunction

$$|LP\rangle = A_{LP}|1\rangle \otimes |G_1\rangle \otimes ... \otimes |G_N\rangle \otimes |G^i_{PDA}\rangle \otimes ... +$$
$$+ \frac{B_{LP}}{\sqrt{N}} \sum_j |0\rangle \otimes |G_1\rangle \otimes ... \otimes |E_j\rangle \otimes ... \otimes |G_N\rangle \otimes |G^i_{PDA}\rangle \otimes ...$$

- upper polariton state with transition frequency $\omega_{UP} = \frac{\omega_0 + \omega_p}{2} + \sqrt{\frac{(\omega_0 - \omega_p)^2}{4} + \Omega^2 N}$ and the wavefunction

$$|UP\rangle = A_{UP}|1\rangle \otimes |G_1\rangle \otimes ... \otimes |G_N\rangle \otimes |G^i_{PDA}\rangle \otimes ... -$$
$$- \frac{B_{UP}}{\sqrt{N}} \sum_j |0\rangle \otimes |G_1\rangle \otimes ... \otimes |E_j\rangle \otimes ... \otimes |G_N\rangle \otimes |G^i_{PDA}\rangle \otimes ...$$

where $A_{LP} = \frac{|\omega_{LP} - \omega_0|}{\sqrt{(\omega_{LP} - \omega_0)^2 + \Omega^2 N}}$ and $B_{LP} = \frac{\Omega}{\sqrt{(\omega_{LP} - \omega_0)^2 + \Omega^2 N}}$ are Hopfield coefficients for lower polariton, whereas $A_{UP} = \frac{|\omega_{UP} - \omega_0|}{\sqrt{(\omega_{UP} - \omega_0)^2 + \Omega^2 N}}$ and $B_{UP} = -\frac{\Omega}{\sqrt{(\omega_{UP} - \omega_0)^2 + \Omega^2 N}}$ are Hopfield coefficients for upper polariton. These coefficients describe the relative weight of the plasmon ($|A_{LP}|^2, |A_{UP}|^2$) or molecule ($|B_{LP}|^2, |B_{UP}|^2$) parts of polariton.[18-19]

It is known that polariton frequencies $\omega_{LP,UP}$ are additionally affected by the concentration quenching,[20] but at dye concentrations $2.5 \times 10^{18}\, cm^{-3}$ these effects are insignificant.[20]

Using the expressions for lower and upper polariton frequencies we obtain that $\lambda_{LP} \approx 880$ nm, $\lambda_{UP} \approx 770$ nm. We note that the incoherent pumping occurs at 780 nm. Because of this detuning, the pumping of both the lower and the upper polariton is inhibited. Dark states have a weak interaction with pumping since they are characterized by a dipole moment close to zero, therefore, the pumping of these states can be neglected. However, dephasing process in dye molecules ensures a probability flow between polaritonic states and dark states, therefore, dark states are populated despite not being pumped directly. Thus, we conclude that in the limit of small pumping rates, the only populated states are the ground state $|G\rangle$, states with an excited PDA level $|PDA_i\rangle$, the LP state $|LP\rangle$, the UP state $|UP\rangle$, and dark states $|D_i\rangle$.

Similar to the Section 1 in Supplementary Materials, the interaction of the system "plasmonic nanoparticle + dye molecules" with the environment leads to transitions between eigenstates. The reservoir Hamiltonian in this case consists of Hamiltonians from six separate reservoirs:

$$\hat{H}_R = \hat{H}_R^{rad} + \hat{H}_R^n + \hat{H}_R^J + \hat{H}_R^{deph} + \hat{H}_R^{pump} + \hat{H}_{SR}^{PDA} \quad \text{(S12)}$$

The first term in Equation S12 is the Hamiltonian of the EM field modes of free space, $\hat{H}_R^{rad} = \sum_{\mathbf{k},\lambda} \hbar \omega_{\mathbf{k}} \hat{c}^\dagger_{\mathbf{k},\lambda} \hat{c}_{\mathbf{k},\lambda}$, similar to the first term in Equation S3. However, the Hamiltonian of the

interaction of the reservoirs with the system has a different form because the plasmonic particle has its own dipole moment: [2-3]

$$\hat{H}_{SR}^{rad} = \sum_{\mathbf{k},\lambda} \hbar(\kappa_{\mathbf{k},\lambda,pl}^{rad} \hat{a}^{\dagger} + \kappa_{\mathbf{k},\lambda,dye}^{rad} \sum_j \hat{\sigma}_j^{\dagger}) \hat{c}_{\mathbf{k},\lambda} + h.c. \quad \text{(S13)}$$

where $\kappa_{\mathbf{k},\lambda,p}^{rad} = -\mathbf{d}_p \mathbf{E}_{\mathbf{k},\lambda}\left(\mathbf{r}_{pl}\right)/\hbar$ and $\kappa_{\mathbf{k},\lambda,dye}^{rad} = -\mathbf{d}_{dye} \mathbf{E}_{\mathbf{k},\lambda}\left(\mathbf{r}_{dye}\right)/\hbar$ are the characteristic interaction rate between the EM field and the plasmon and the dye, respectively; and $d_p = \left|\mathbf{d}_p\right|$ is the matrix element of dipole transitions from plasmon excited state to the ground state. The d_p is estimated as $\sim 1400D$.[20-21]

The second term is responsible for the nonradiative decay of the dye molecule and is of the form $\hat{H}_R^n = \sum_{\mathbf{k},\lambda} \hbar\omega_{\mathbf{k}} \hat{f}_{\mathbf{k},\lambda}^{\dagger} \hat{f}_{\mathbf{k},\lambda}$. Its interaction term is given in equation (5). This term is insignificant for molecules in the vicinity of plasmonic nanoparticle, since the nonradiative decay of LP is mainly due to ohmic losses in the metal of the plasmonic nanoparticle. Therefore, this term is omitted from the Lindblad equation for dye molecules in the vicinity of plasmonic nanoparticle.

Ohmic losses are described by the third term, representing the phonon bath, $\hat{H}_R^J = \sum_j \hbar\omega_j \hat{r}_j^{\dagger} \hat{r}_j$. The operators $\hat{r}_j$ and $\hat{r}_j^{\dagger}$ correspond to the relaxation and excitation of a phonon with frequency ω_j in the metal. The interaction of this reservoir with the system is: [2-3]

$$\hat{H}_{SR}^J = \sum_j \hbar\kappa_j^J \hat{a}^{\dagger} \hat{r}_j + h.c. \quad \text{(S14)}$$

The interaction constant between *j*-th phonon mode and the plasmon is equal to κ_j^J.

The fourth term in (12) is the Hamiltonian of the vibronic degrees of freedom of PDA, $\hat{H}_R^{deph} = \sum_j \hbar\omega_j \hat{b}_j^{\dagger} \hat{b}_j$. The interaction Hamiltonian is similar to the analogous term in Equation S6: [2-3]

$$\hat{H}_{SR}^{deph} = \sum_j \hbar(\hat{b}_j^{\dagger} + \hat{b}_j) \sum_{k,n} \kappa_{jnk}^{deph} \left|k\right\rangle\left\langle n\right| + h.c., \quad \text{(S15)}$$

where $\left|k\right\rangle$ is either $\left|E_i\right\rangle$ or $\left|PDA_i\right\rangle$ or $\left|1\right\rangle$.

The fifth term in Equation S12 is the Hamiltonian of the pump reservoir, $\hat{H}_R^{pump} = \sum_j \hbar\omega_j \hat{p}_j^{\dagger} \hat{p}_j$. In the case of molecules arranged in the dielectric nanoparticle the pump reservoir interacts both the electronic degree of freedom of the molecule and the plasmonic particle as: [2-3]

$$\hat{H}_{SR}^{pump} = \sum_j \hbar(\kappa_{j,pl}^{pump} \hat{a}^{\dagger} + \kappa_{j,dye}^{pump} \sum_i \hat{\sigma}_i^{\dagger}) \hat{p}_j + h.c. \quad \text{(S16)}$$

with the interaction constants $\kappa_{j,pl}^{pump}$ and $\kappa_{j,dye}^{pump}$. Similar to Equation S13 the terms with $\kappa_{j,dye}^{pump}$ multiplier can be neglected.

The sixth term in Equation S12 represents optical phonons in PDA can be effectively described by the Hamiltonian $\hat{H}_R^{PDA} = \sum_j \hbar\omega_j \hat{q}_j^{\dagger} \hat{q}_j$, i.e. reservoir of two-level systems with transition frequencies ω_j and positive population inversion. This reservoir describes the non-radiative decay

of PDA states. $\hat{q}_j$ and $\hat{q}_j^\dagger$ are transition operators to the ground state and the excited state of *j*-th two-level system, respectively. Hamiltonian of the interaction of this reservoir with the system has the form:

$$\hat{H}_{SR}^{PDA} = \sum_j \sum_i \hbar \kappa_j^{PDA} \hat{s}_i^\dagger \hat{q}_j + h.c. \tag{S17}$$

with the interaction constant κ_j^{PDA}.

Now, we use the Born-Markov approximation to exclude the reservoir variables and obtain the Lindblad equation for the density matrix of the system: [5]

$$\frac{\partial \hat{\rho}}{\partial t} = -\frac{i}{\hbar}\left[\hat{H}_S, \hat{\rho}\right] + \hat{L}_{rad}(\hat{\rho}) + \hat{L}_J(\hat{\rho}) + \hat{L}_{PDA}(\hat{\rho}) + \hat{L}_{deph}(\hat{\rho}) + \hat{L}_{pump}(\hat{\rho}) \tag{S18}$$

$\hat{L}_i(\hat{\rho})$ are the Lindblad superoperators having the form

$$\hat{L}_{rad}(\hat{\rho}) \approx \frac{\gamma_{rad}^p}{2}\left(2\hat{a}\hat{\rho}\hat{a}^\dagger - \hat{a}^\dagger\hat{a}\hat{\rho} - \hat{\rho}\hat{a}^\dagger\hat{a}\right)$$

$$\hat{L}_J(\hat{\rho}) = \frac{\gamma_n^p}{2}\left(2\hat{a}\hat{\rho}\hat{a}^\dagger - \hat{a}^\dagger\hat{a}\hat{\rho} - \hat{\rho}\hat{a}^\dagger\hat{a}\right)$$

$$\hat{L}_{PDA}(\hat{\rho}) = \frac{\tilde{\gamma}_n}{2}\sum_i\left(2\hat{s}_i\hat{\rho}\hat{s}_i^\dagger - \hat{s}_i^\dagger\hat{s}_i\hat{\rho} - \hat{\rho}\hat{s}_i^\dagger\hat{s}_i\right)$$

$$\hat{L}_{deph}(\hat{\rho}) = \sum_{i,j}\frac{\gamma_{ph}}{2}\left(2\hat{S}_i^\dagger\hat{S}_j\hat{\rho}\hat{S}_j^\dagger\hat{S}_i - \hat{S}_j^\dagger\hat{S}_i\hat{S}_i^\dagger\hat{S}_j\hat{\rho} - \hat{\rho}\hat{S}_j^\dagger\hat{S}_i\hat{S}_i^\dagger\hat{S}_j\right)$$

$\hat{S}_i$ is either $\hat{s}_k, k = 1,...$ or $\hat{\sigma}_k, k = 1,...$ or $\hat{a}$.

$$\hat{L}_{pump}(\hat{\rho}) = \frac{\gamma_{pump}^p}{2}\left(2\hat{a}^\dagger\hat{\rho}\hat{a} - \hat{a}\hat{a}^\dagger\hat{\rho} - \hat{\rho}\hat{a}\hat{a}^\dagger\right)$$

Here $\hat{L}_{rad}(\hat{\rho})$ describes the radiative decay in the "molecules in plasmonic nanoparticle" system; $\hat{L}_J(\hat{\rho})$ describes the non-radiative decay in the "molecules in plasmonic nanoparticle" system; $\hat{L}_{PDA}(\hat{\rho})$ describes nonradiative decay of PDA states; $\hat{L}_{deph}(\hat{\rho})$ describes dephasing of dye molecules polarization and plasmon polarization within the PDA; $\hat{L}_{pump}(\hat{\rho})$ describes the incoherent pumping of plasmon.

Let us summarize relaxation processes and all possible transitions described by Equation S18. First relaxation process is the relaxation of energy in the plasmonic nanoparticles due to ohmic and radiation losses. This relaxation process leads to energy transitions between states $|LP\rangle \to |G\rangle$, $|UP\rangle \to |G\rangle$. Since these two rates are much faster than the relaxation rates of the population inversion of the dye molecules,[12, 22] the latter can be neglected. Second relaxation process is the relaxation of the population inversion of PDA states across nonradiative transitions. We assume that PDA decays nonradiative. This process leads to the transition from the PDA states to the ground state, $|PDA_i\rangle \to |G\rangle$. Third relaxation process is the dephasing processes in the dye

molecules and plasmon particle that lead to destruction of the polarizations phases and cause transitions between the lower polariton, $|LP\rangle$, the upper polariton, $|UP\rangle$, the dark states $|D_i\rangle$, and the PDA states, $|PDA_i\rangle$. Finally, the optical pumping of the system leading to transitions $|G\rangle \to |LP\rangle$, $|G\rangle \to |UP\rangle$. All processes are shown schematically in Fig. 1b in the main text.

The important question is to determine the rates γ_i^{nm} in Equation S18. Since LP and UP states are a mix of molecular and plasmonic excitations, all transition rates associated with them are modified by Hopfield coefficients A_{LP}, B_{LP}, A_{UP} or B_{UP} (see Equation S19 for more detail). Numerically, these values are determined from the expression for the LP state and UP state. The radiation relaxation rate of the plasmonic nanoparticle can be determined from its dipole moment as $\gamma_{rad}^{p} = \frac{4\omega_0^3 d_p^2}{3\hbar c^3}$. Ohmic losses in the plasmonic nanoparticle, γ_{rad}^{n}, can be determined through the characteristic volume of the plasmonic particle and dielectric permittivity of gold and PDA.[12, 22] The dephasing rate γ_{ph}^{p} that leads to transition plasmonic states to PDA states can be found from the difference between the linewidth of plasmonic nanoparticle in absence of PDA shell and the linewidth of plasmonic nanoparticle within PDA shell. The pumping rate γ_{pump}^{p} is estimated based on the intensity of the pumping laser (see details in Section 3 in Supplementary materials).

Ultimately, Eq. (S18) and the corresponding rates (see Table S2) are sufficient to write the kinetic equations. Similar to Section 1 in Supplementary materials, the rates of the above processes are determined using Fermi's golden rule with numerical values from experimental data.

The kinetic equations describing the transition between the energy levels of the system are of the form:

$$\begin{aligned}
\dot{n}_{UP} &= -|A_{UP}|^2(\gamma_{rad}^{p} + \gamma_{n}^{p})n_{UP} + |A_{UP}|^2 \gamma_{pump}^{UP} n_G - (|B_{UP}|^2 \gamma_{ph} + |A_{UP}|^2 \gamma_{ph}^{p})n_{UP} - \\
&-(\gamma_a |A_{LP}A_{UP}|^2 + \gamma_\sigma |B_{LP}B_{UP}|^2 + \sqrt{\gamma_\sigma \gamma_a}(|A_{LP}B_{UP}|^2 + |A_{UP}B_{LP}|^2))n_{UP} - \\
&-N\gamma_\sigma |A_{UP}|^2 n_{UP} + (|B_{UP}|^2 \tilde{\gamma}_{ph} + |A_{UP}|^2 \tilde{\gamma}_{ph}^{p})n_{PDA}
\end{aligned}$$

$$\dot{n}_D = -\gamma_{ph} n_D + N\gamma_\sigma |A_{UP}|^2 n_{UP} - |B_{LP}|^2 \gamma_\sigma n_D$$

$$\begin{aligned}
\dot{n}_{LP} &= -|A_{LP}|^2(\gamma_{rad}^{p} + \gamma_{n}^{p})n_{LP} + |A_{LP}|^2 \gamma_{pump}^{LP} n_G - (|B_{LP}|^2 \gamma_{ph} + |A_{LP}|^2 \gamma_{ph}^{p})n_{LP} + \\
&+(|B_{LP}|^2 \tilde{\gamma}_{ph} + |A_{LP}|^2 \tilde{\gamma}_{ph}^{p})n_{PDA} + |B_{LP}|^2 \gamma_\sigma n_D + \\
&+(\gamma_a |A_{LP}A_{UP}|^2 + \gamma_\sigma |B_{LP}B_{UP}|^2 + \sqrt{\gamma_\sigma \gamma_a}(|A_{LP}B_{UP}|^2 + |A_{UP}B_{LP}|^2))n_{UP}
\end{aligned}$$

$$\begin{aligned}
\dot{n}_{PDA} &= \gamma_{ph} n_D + (|B_{LP}|^2 \gamma_{ph} + |A_{LP}|^2 \gamma_{ph}^{p})n_{LP} + (|B_{UP}|^2 \gamma_{ph} + |A_{UP}|^2 \gamma_{ph}^{p})n_{UP} - \\
&-(|B_{LP}|^2 \tilde{\gamma}_{ph} + |A_{LP}|^2 \tilde{\gamma}_{ph}^{p})n_{PDA} - \tilde{\gamma}_n n_{PDA} - (|B_{UP}|^2 \tilde{\gamma}_{ph} + |A_{UP}|^2 \tilde{\gamma}_{ph}^{p})n_{PDA}
\end{aligned}$$

$$\begin{aligned}
\dot{n}_G &= |A_{LP}|^2(\gamma_{rad}^{p} + \gamma_{n}^{p})n_{LP} + |A_{UP}|^2(\gamma_{rad}^{p} + \gamma_{n}^{p})n_{UP} - |A_{LP}|^2 \gamma_{pump}^{LP} n_G - \\
&-|A_{UP}|^2 \gamma_{pump}^{UP} n_G + \tilde{\gamma}_n n_{PDA}
\end{aligned} \qquad \text{(S19)}$$

where n_{LP}, n_{UP} and n_G are the populations of the LP, UP and ground states, respectively. The n_{PDA} is the sum of the populations of the PDA states. The n_D is the sum of the populations of dark states. The γ_{rad}^{p} is the radiative relaxation rate of the plasmon; γ_{n}^{p} is the nonradiative relaxation rate of the plasmon. γ_{pump}^{LP} and γ_{pump}^{UP} is the pump rate from $|G\rangle$ to $|LP\rangle$ and from $|G\rangle$ to $|UP\rangle$, respectively. The γ_{ph} and γ_{ph}^{p} are dephasing rates associated with dye molecules and plasmonic particle, respectively; $\tilde{\gamma}_{ph}$ and $\tilde{\gamma}_{ph}^{p}$ is the rate of inverse transition from the PDA state to LP and UP. $\tilde{\gamma}_{ph} = \gamma_{ph} \exp[-\hbar(\omega_0 - \langle\omega_{PDA}\rangle)/kT]/N_{PDA}$ (similar to the system with dielectric particle, see Section 4.1). Note that neither N_{PDA} not $\langle\omega_{PDA}\rangle$ need to be determined, instead, the factor $\exp[-\hbar(\omega_0 - \langle\omega_{PDA}\rangle)/kT]/N_{PDA}$ is used as an optimization factor for both the system with the dielectric particle and the plasmon system. For the sake of simplicity, the transition rate from PDA levels to plasmon level, $\tilde{\gamma}_{ph}^{p}$, is assumed to be modified by same factor as the transition rate from PDA to dye molecule excited state $\tilde{\gamma}_{ph}$, namely, $\tilde{\gamma}_{ph}^{p} = \gamma_{ph}^{p} \times \tilde{\gamma}_{ph} / \gamma_{ph}$. A more accurate model can be developed if we consider the structure of energy levels in PDA and all the transition rates within. However, this approach is excessively complex. $\tilde{\gamma}_{n}$ is the non-radiative decay rate of the PDA states into the ground state $|G\rangle$. The $|A_{LP}|^2 = 0.61$ is the fraction of plasmon state in LP, $|B_{LP}|^2 = 0.39$ is the fraction of excited dye states in LP. The $|A_{UP}|^2 = 0.39$ is the fraction of plasmon state in UP, $|B_{UP}|^2 = 0.61$ is the fraction of excited dye states in UP. Each term in equation (5) represents the corresponding relaxation rate depicted in Fig. 1b.

Equations S19 allow us to determine the effective fluorescence cross section of dye molecules in plasmonic nanoparticle compared to a free molecule of Cy-7.5 dye. To do this, we determine the steady-state value of radiating state populations, n_{LP} and n_{UP}, from Equation S19. The fluorescence intensity is determined by the radiation relaxation rate of the plasmonic particle γ_{rad}^{p} and the population of LP and UP. Unlike the dielectric nanoparticle with dye molecules, the plasmonic system acts as a single emitter.

Section 3 Estimate of probability of excitations of different states in the pumped nano-mesoscopic systems

In this section, we estimate probability of excitations for Cy-7.5 dye molecules in PDA shell without plasmonic nanoparticle, as well as the probability of excitations for lower polariton (LP) and upper polariton (UP) in the Core-Shell plasmonic nanoparticle. These probabilities determine the fraction of Cy-7.5 molecules in the excited states and the fraction of hybrid nanoparticles which are in LP and UP states, respectively.

The probability of excitations in the system is determined by the pump power and relaxation rates. The relaxation rates are established experimentally from fluorescence decay rates (see Fig. 2 in the main text). The pumping rate can be calculated using the established formula for the imaginary part of dielectric constant of the active medium:

$$\mathrm{Im}(\varepsilon) = 4\pi \frac{d_{dye}^2 n}{\hbar \gamma_\sigma},$$

where n – is the concentration of active atoms. From this expression we can estimate the absorption cross section of a single molecule of the active medium and find for given values of γ_{ph}, d_{dye}, n and continuous pump power 1 kW/cm^2 that the probability of an individual Cy-7.5 molecule excitation in dielectric nanoparticle is 2×10^{-2}, and $\gamma_{pump} \approx 2\times10^{-2}(\gamma_{rad}+\gamma_n) \ll \gamma_{rad}+\gamma_n$.

A similar estimate can be made for the NP-dye molecules system. Since the dipole moment of the Au nanorod (estimated as $1400D$ from dimensions) is approximately 100 times larger than the dipole moment of dye molecules (approximately $13D$), the emission rates for plasmonic nanorod are 10^4 faster than those for a dye molecule. The absorption rate benefits from larger dipole moment as well, however, due to the frequency shift of the LP compared to the excited state of the molecule, the pumping becomes less efficient proportional to Lorenz factor $(\gamma_{LP}/2)^2 / \left[(\gamma_{LP}/2)^2 + (\omega_{pump}-\omega_{LP})^2\right]$, where γ_{LP} is the linewidth of the LP and ω_{pump} is the frequency of the incoherent pumping (the system is pumped at 780 nm). Moreover, the pump rate is further decreased by the fact that the polarization of plasmonic nanoparticle may not coincide with the polarization of pumping light. Averaging over all possible polarizations yields a factor of $1/3$. Thus, we estimate probability of excitation of LP state as 3×10^{-5} and corresponding pump rate $\gamma_{pump}^{LP} \approx 3\times10^{-5}(\gamma_{rad}^p+\gamma_n^p) \ll \gamma_{rad}^p+\gamma_n^p$. Similar estimate can be done for UP, which yields probability of excitation of UP state 5×10^{-5} and pump rate $\gamma_{pump}^{UP} \approx 5\times10^{-5}(\gamma_{rad}^p+\gamma_n^p) \ll \gamma_{rad}^p+\gamma_n^p$.

Table S1. List of transition rates between the energy levels for the silica structure

Transition from «1st state» to «2nd state»	Rate of forward transition
Excited dye state $\rightarrow$ ground state	$\gamma_{E\to G} = \gamma_{rad} + \gamma_n$
PDA states $\rightarrow$ ground state	$\gamma_{PDA\to G} = \tilde{\gamma}_n$
PDA states $\rightarrow$ excited dye state	$\gamma_{PDA\to E} = \tilde{\gamma}_{ph}$
Excited dye state $\rightarrow$ PDA states	$\gamma_{E\to PDA} = \gamma_{ph}$
Ground state $\rightarrow$ Excited dye state	$\gamma_{G\to E} = \gamma_{pump}$

Table S2. The values of the relaxation rates and frequencies in systems under consideration

$\gamma_{pump} = 1.1\times10^{-9}\omega_0$	$\gamma_{rad} = 4.7\times10^{-8}\omega_0$	$\gamma_n = 4.2\times10^{-7}\omega_0$	$\gamma_{ph} = 3\times10^{-2}\omega_0$	$\tilde{\gamma}_{ph} = 3\times10^{-8}\omega_0$
$\gamma_\sigma = 6\times10^{-2}\omega_0$	$\gamma_a = 0.18\omega_0$	$\tilde{\gamma}_n = 1.5\times10^{-5}\omega_0$	$\gamma_{ph}^p = 0.14\omega_0$	$\tilde{\gamma}_{ph}^p = 1.4\times10^{-7}\omega_0$
$\gamma_{pump}^{LP} = 2.9\times10^{-7}\omega_0$	$\gamma_{pump}^{UP} = 4.6\times10^{-7}$	$\gamma_{rad}^p = 4.6\times10^{-4}\omega_0$	$\gamma_n^p = 8.3\times10^{-3}\omega_0$	
$\omega_0 = 2.33\times10^{15}\,c^{-1}$		$\omega_p = 2.26\times10^{15}\,c^{-1}$		

Section 4 Measurements of the concentration of dye molecules in the shell of plasmonic nanoparticles on the PDA shell unquenching effect

Figure S1 shows the results of the measured dependence of the "PDA shell unquenching" effect on the concentration of dye molecules in the nanoparticle shell. The effect is shown as the ratio of the measured fluorescence signal of a single plasmonic nanoparticle to that of a single dielectric nanoparticle both surrounded by PDA shell embedded with Cy 7.5. For each concentration, the fluorescence of seven different pairs of dielectric and plasmonic nanoparticles is shown. As can be clearly seen from the figure, the maximum "unquenching" effect is realized for the concentration of dye molecules in the shell $2.5\times10^{18} cm^{-3}$.

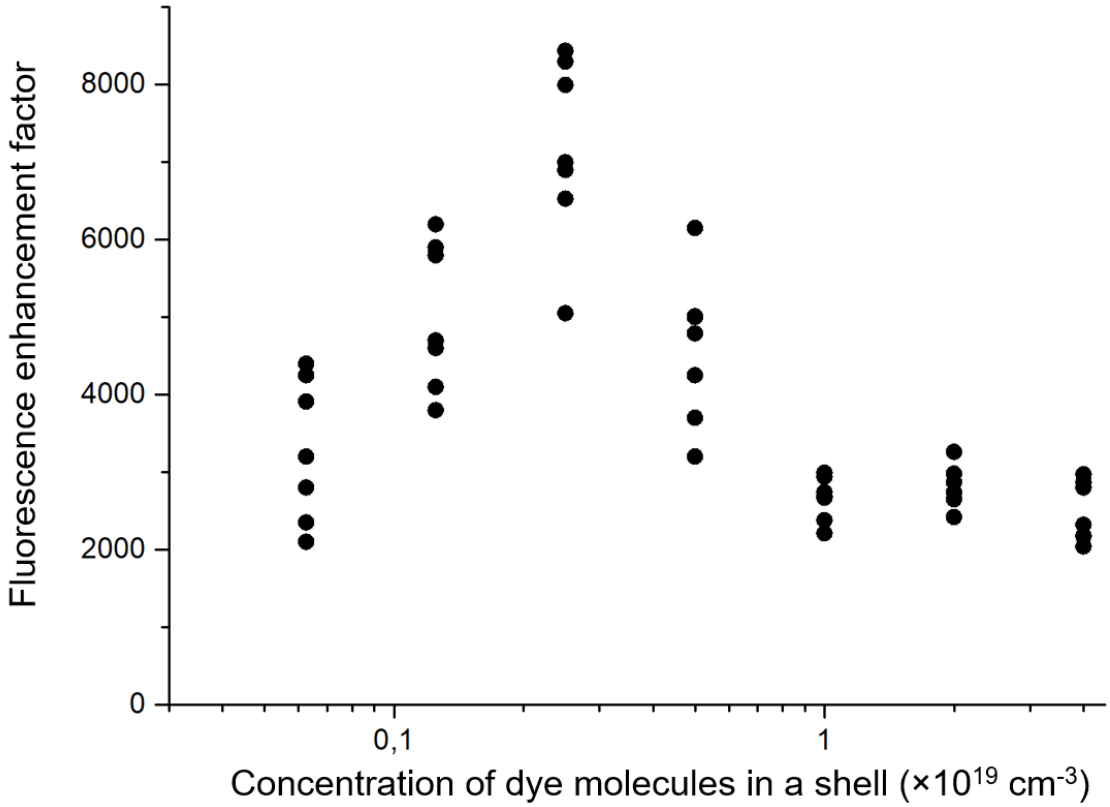

Figure S1. Dependence of the "PDA shell unquenching" effect on the concentration of dye molecules in the nanoparticle shell. The effect is presented as the ratio of the measured fluorescence signal of a single plasmonic nanoparticle to that of a single dielectric nanoparticle. For each concentration, the fluorescence of seven different pairs of dielectric and plasmonic nanoparticles is presented.

Section 5 Modeling of extinction spectra

In this section we demonstrate qualitative description of extinction spectra of dye-plasmon system. We assume that there are two molecule states interacting with the plasmonic particle per Cy 7.5 dye molecule responsible for two peaks in Figure 2c. The reason why only one state is considered in Sections 1-2 of Supplementary materials is because only one state participates in emission process. With two states interacting with the plasmon nanoparticle, the Hamiltonian becomes:

$$\hat{H}_2 = \hbar\omega_0 \sum_j \hat{\sigma}_j^\dagger \hat{\sigma}_j + \hbar(\omega_0 + \Delta\omega_0) \sum_j \hat{\tilde{\sigma}}_j^\dagger \hat{\tilde{\sigma}}_j + \hbar\omega_p \hat{a}^\dagger \hat{a} + \\ + \hbar\tilde{\Omega}_R \sum_j (\hat{a}\hat{\sigma}_j^\dagger + \hat{a}^\dagger \hat{\sigma}_j) + \hbar\tilde{\Omega}_R \sum_j (\hat{a}\hat{\tilde{\sigma}}_j^\dagger + \hat{a}^\dagger \hat{\tilde{\sigma}}_j) \quad \text{(S20)}$$

where $\omega_0 + \Delta\omega_0$ is Cy 7.5 dye absorption frequency estimated from experimental data, see Figure 2c from the main text, $\Delta\omega_0 \approx 2.5\times10^{14} c^{-1}$; $\tilde{\Omega}_R \approx 1.4\times10^{14} c^{-1}$ is the adjusted interaction constant determined in such way that results in the same detuning of $2.38\times10^{14} c^{-1}$ between emitting LP and UP states as Equation (S11).

Using Eq. (S20) we can determine the transition frequencies of the Core-Shell system, as well as their linewidth, from Table (S2). The resulting spectra, and their comparison to experimetal data are depicted in Figures S2-S3.

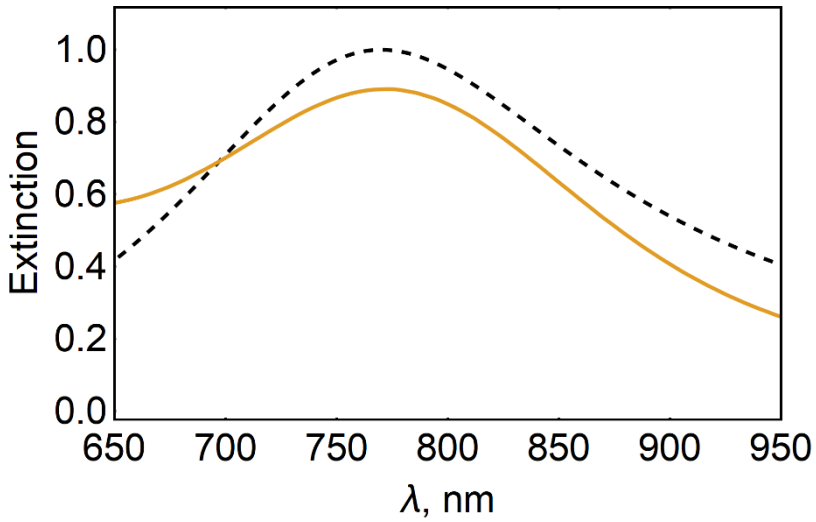

Figure S2. Comparison between experimental extinction spectrum (solid orange curve) and theoretically predicted spectrum (dashed black curve) in core-shell nanoparticle without dye molecules (Au nanorod surrounded by PDA shell).

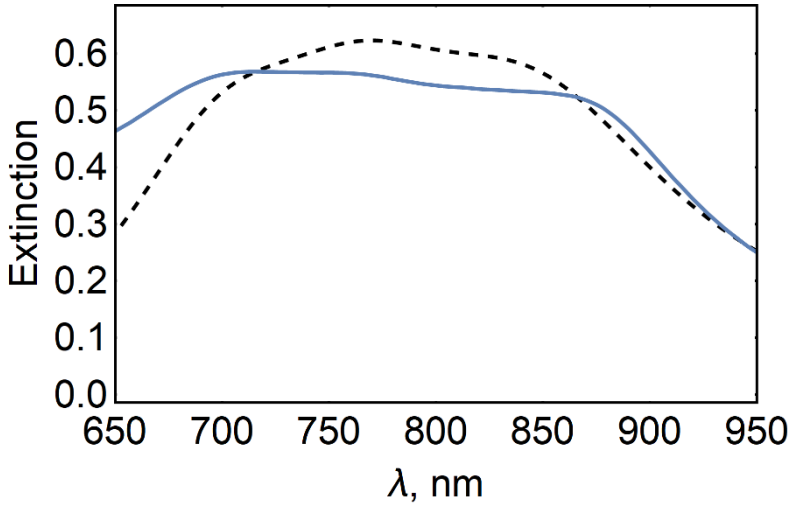

Figure S3. Comparison between experimental extinction spectrum (solid blue curve) and theoretically predicted spectrum (dashed black curve) in core-shell nanoparticle with Cy 7.5 dye molecules (Au nanorod surrounded by PDA shell with embedded Cy 7.5 molecules).

Section 6 Estimates of energy splitting in the hybrid system

We start by estimating coupling strength between dye molecules and plasmon NP as $2\sqrt{\hbar^2\left(\omega_p-\omega_0\right)^2/4+\Omega_0^2}$ where the first term inside the square root describes splitting in absence of interaction and $\Omega_0^2=\sum_i\left|\mathbf{E}_0(\mathbf{r}_i)\mathbf{d}_{dye}\right|^2$ is splitting due to the interaction [23-24]. Here $\left|\mathbf{E}_0(\mathbf{r}_i)\right|=f(\mathbf{r}_i)\sqrt{\frac{4\pi\hbar\omega}{V_{mode}}}$ is electric field 'per one plasmon' [5, 25], $f(\mathbf{r}_i)$ is normalized ($f(\mathbf{r})=\left|\mathbf{E}_0(\mathbf{r})\right|/\max\left|\mathbf{E}_0(\mathbf{r})\right|$) spatial field distribution of the plasmon mode at location of each dye molecule, $\mathbf{r}_i$, V_{mode} is the plasmon mode volume, $V_{mode}=\int\left|\mathbf{E}_0(\mathbf{r})\right|^2d^3\mathbf{r}/\max\left|\mathbf{E}_0(\mathbf{r})\right|^2$ [26]. Supposing that the dipole moments of dye molecules are oriented parallel to the plasmon electric field, the expression for coupling strength can be simplified to $\sqrt{\frac{4\pi\hbar\omega}{V_{mode}}}\left|\mathbf{d}_{dye}\right|\sqrt{\sum_i\left|f(\mathbf{r}_i)\right|^2}$. The expression under square root sign is very similar to normalization condition, which is what we intend to exploit. We transition from sum to integral as follows:

$$\sum_i\left|f(\mathbf{r}_i)\right|^2=\rho\sum_i\Delta V\left|f(\mathbf{r}_i)\right|^2\approx\rho\int_{shell}\left|f(\mathbf{r})\right|^2d^3\mathbf{r}$$

where ΔV is volume per one dye molecule (that is small enough to assume that the field is approximately constant inside this volume), and ρ is dye concentration (evidently, $\rho=1/\Delta V$). We assume that the plasmonic mode lies almost entirely within PDA shell with embedded dye molecules. In this case $\int_{shell}\left|f(\mathbf{r})\right|^2d^3\mathbf{r}\approx\int\left|f(\mathbf{r})\right|^2d^3\mathbf{r}=V_{mode}$. Inserting this into the expression for coupling strength yields $\sqrt{4\pi\hbar\omega\rho}\left|\mathbf{d}_{dye}\right|$.

To obtain energy splitting we take into account the initial frequency detuning between the mode and active molecules [23]. This results in the following expression: $2\sqrt{\frac{\hbar^2(\omega_p-\omega_0)^2}{4}+4\pi\hbar\omega\rho\left|\mathbf{d}_{dye}\right|^2}$, where the first addend inside the square root describes splitting in absence of interaction, and '2' in front stands for two energy levels shifting in the opposite directions (similar to trivial resonant case where the splitting is the interaction strength times two [27]. Inserting all the numbers: $\hbar(\omega_0-\omega_p)=46\text{meV}$, $\hbar\omega=1.48\times10^3\text{meV}$, $d_{dye}=13D=1.3\times10^{-17}CGS$, $\rho=2.5\times10^{18}cm^{-3}$, $\left|\mathbf{d}_{dye}\right|^2\rho\approx0.26\text{meV}$, we obtain the resulting splitting 146meV. Note that the first term in the square root contributes little to the final result, and the splitting is mostly attributed to interaction strength.

Section 7 Quantity of SERS signal in the measured spectra

In this section we show results of our fluorescent measurements for the different samples: (a) Core-Shell plasmonic nanoparticle, (b) Core-Shell dielectric nanoparticle, (c) nanorods without shell. The dielectric core-shell nanostructure consists of a silica core with a diameter of about 50 nm and a shell of 5 nm thick PDA with Cy 7.5 molecules. The plasmonic hybrid core-shell nanostructure consists of an Au nanorod with a 10 nm thick PDA shell containing Cy 7.5 dye molecules. The Au nanorod has a width of 10 nm and a length of 40 nm, Cy 7.5 dye molecules were embedded in the polymer shell at a concentration of 2.5×10^{18} cm^{-3}. Figure S4 shows the results of fluorescence

measurements for samples excited with CW laser radiation at 780 nm with an intensity of about 1 kW/cm^2. For the fluorescence measurements, a set of long-pass interference filters was used to detect emission at wavelengths above 800 nm.

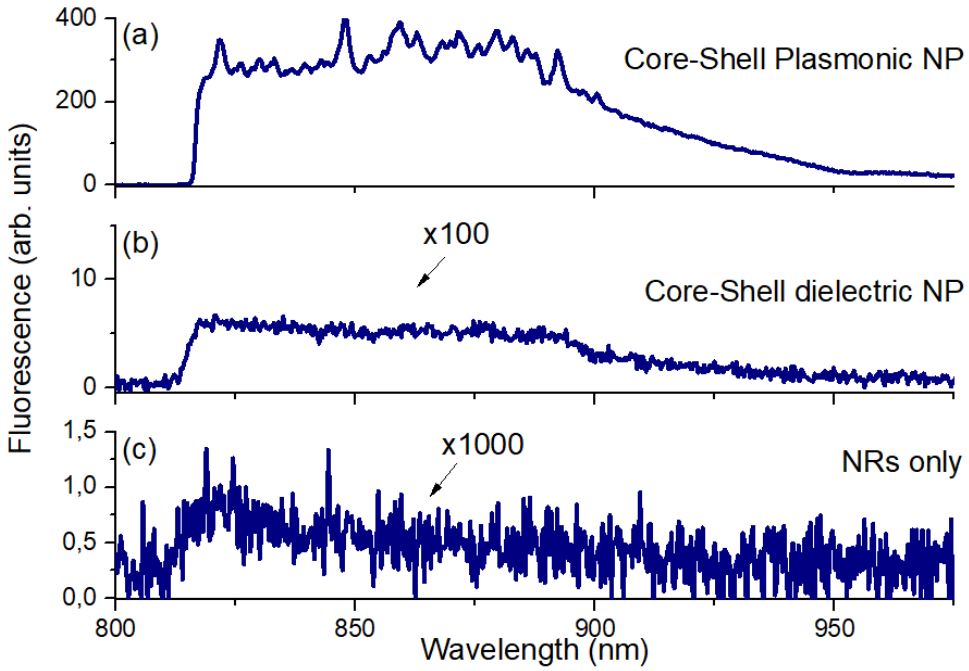

Figure S4. Measuremets of fluorescence signal from three different objects: (a) Core-Shell plasmonic nanoparticle, (b) Core-Shell dielectric nanoparticle, (c) nanorods.

The measurements on Fig. S4 show that the fluorescence of a single plasmonic particle is many orders of magnitude smaller than the resulting emission from NP+dye system. This indicates that the background is not SERS background, but fluorescence. Thus the ratio between the fluorescence signal and the SERS signal in the measured spectrum in Fig. 3a is approximately 11:1. In other words, the signal from SERS accounts for about 8% of the measured signal.

Section 8 Materials and experimental setup

Experimental setup

The experimental setup is based on Nikon Ti-U inverted microscope with 780 nm cw laser for excitation and corresponding filter cube (Semrock BP FF01-775/46-25, dichroic mirror Di03-R785-t3-25x36, notch NF03-785E-25). Laser radiation and fluorescence was focused and collected through the 100x NA 1.49 Oil objective. We used Princeton Instruments EMCCD as 2D detector. For fluorescence lifetime measurements we used PicoHarp 300 TCSPC system with SPAD, which was connected to the microscope through 100 μm fiber as confocal aperture and 780 nm 100 fs pulsed laser for excitation. Extinction spectra were measured using AnalyticJena Specord 200 spectrophotometer.

Sample preparation

Reagents. Dopamine hydrochloride (DA, H8502), Cetyltrimethylammonium bromide (CTAB, > 98.0%), cetyltrimethylammonium chloride (CTAC, 25% water solution), L-ascorbic acid (AA, >99,9), hydrochloric acid (HCl, 37 wt.% in water), tetraethyl orthosilicate (TEOS, 98%), thiolated polyethylene glycol (mPEG-SH, 99%), and sodium borohydride ($NaBH_4$, 99%) were purchased from Sigma-Aldrich. CY7.5–amine was obtained from Lumiprobe. Hydrogen tetrachloroaurate trihydrate ($HAuCl4{\cdot}3H_2O$) and silver nitrate ($AgNO_3$, >99%) were purchased from Alfa Aesar. Ultrapure water obtained from a Milli-Q Integral 5 system was used in all experiments.

Synthesis of AuNRs. Au NRs with diameters of about 10-12 nm were synthesized by a seed-mediated growth method [28] with minor modifications concerning the concentrations of some reagents and reaction protocols. First, seed gold particles are prepared by adding aqueous sodium borohydride (10 mM, 0.6 ml) to a mixed aqueous solution of CTAB (0.1M, 10 ml) and $HAuCl_4$ (10 mM, 0.25 ml). For preparation of AuNRs with the aspect ratio of about 4, 1 ml of 4 mM $AgNO_3$, 2.5 ml of 10 M $HAuCl_4$, 0.5 ml of 80 mM AA, 0.5 ml of 1M HCl, and 0.5 ml of gold seed solutions are sequentially added to 50 ml of 0.1 M CTAB solution. The nanorods are allowed to grow overnight without stirring at 30 °C.

Coating with PDA shell containing different amount of CY7.5. First, the prepared nanorods were PEGilated using procedure described elsewhere [28]. After PEGilation AuNRs were dispersed in water in concentration of 300 µg/mL which correspond to number concentration of 45×10^{11} mL^{-1} (see calculation below). PDA shell were grown on the surface of PEGilated nanorods. Tho this end 1 mL of AuNRs was mixed with 2 mL of water and 300µL of 100 mM Tris buffer (pH=8.5). Dopamine (DA) solutions at initial concentration 5 mg/mL were freshly prepared in water. Next, 100 µL of DA solution was quickly injected into the mixtire and allowed to react for 3 h at the room temperature under continuous stirring (500 rpm). To initiate formation of CY7.5 embedded PDA shell 5, 20 and 80 µL of CY7.5 amine solution in DMSO (1 mg/mL) were added to different batches of nanorod during shell growth process. The as-synthesized PDA coated nanorods with or without CY7.5 was purified by repeated centrifugation at 12000 g for 15 min and finally resuspended in 3 mL of water.

Synthesis of PDA coated silica reference particles. An aliquot (1.5 mL) of 30% ammonia was added to 50 mL of absolute ethanol. The mixture was stirred vigorously, and a subsequent aliquot (1.5 mL, 6.7 mmol) of TEOS was added dropwise. The mixture was allowed to react during 3 hours under stirring (300 rpm). The as-synthesized silica particles were purified by repeated centrifugation at 12000 g for 15 min and finally resuspended in 50 mL of water. The PDA shell was grown according procedure presented above without significant modifications.

References

1. Zou, Y.; Chen, X.; Yang, P.; Liang, G.; Yang, Y.; Gu, Z.; Li, Y., Regulating the absorption spectrum of polydopamine. *Sci. Adv.* **2020,** *6* (36), eabb4696.
2. Scully, M. O.; Zubairy, M. S., *Quantum optics*. Cambridge University Press: Cambridge, UK, 1997.
3. Carmichael, H. J., *Statistical methods in quantum optics 1: master equations and Fokker-Planck equations*. Springer Science & Business Media: New York, 2013.
4. Kubo, R., Statistical-mechanical theory of irreversible processes. I. General theory and simple applications to magnetic and conduction problems. *J. Phys. Soc. Jpn.* **1957,** *12*, 570-586.
5. Shishkov, V. Y.; Andrianov, E.; Pukhov, A.; Vinogradov, A., Hermitian description of localized plasmons in dispersive dissipative subwavelength spherical nanostructures. *Physical Review B* **2016,** *94* (23), 235443.

6. Kosloff, R., Quantum thermodynamics: A dynamical viewpoint. *Entropy* **2013,** *15*, 2100–2128.
7. Haag, R.; Hugenholtz, N. M.; Winnink, M., On the equilibrium states in quantum statistical mechanics. *Commun. Math. Phys.* **1967,** *5*, 215-236.
8. Martin, P. C.; Schwinger, J., Theory of many-particle systems I. *Phys. Rev.* **1959,** *115*, 1342.
9. Tame, M. S.; McEnery, K.; Özdemir, Ş.; Lee, J.; Maier, S. A.; Kim, M., Quantum plasmonics. *Nature Physics* **2013,** *9* (6), 329-340.
10. Tavis, M.; Cummings, F. W., Approximate solutions for an N-molecule-radiation-field Hamiltonian. *Phys. Rev.* **1969,** *188* (2), 692.
11. Tavis, M.; Cummings, F. W., Exact solution for an N-molecule—radiation-field Hamiltonian. *Phys. Rev.* **1968,** *170* (2), 379.
12. Klimov, V. V., *Nanoplasmonics*. CRS press: 2014.
13. Johnson, P. B.; Christy, R.-W., Optical constants of the noble metals. *Physical review B* **1972,** *6* (12), 4370.
14. Bohren, C. F.; Huffman, D. R., *Absorption and scattering of light by small particles*. John Wiley & Sons: 2008.
15. Bernsmann, F.; Ersen, O.; Voegel, J. C.; Jan, E.; Kotov, N. A.; Ball, V., Melanin-containing films: growth from dopamine solutions versus layer-by-layer deposition. *ChemPhysChem* **2010,** *11* (15), 3299-3305.
16. Vega, M.; Martín del Valle, E. M.; Pérez, M.; Pecharromán, C.; Marcelo, G., Color engineering of silicon nitride surfaces to characterize the polydopamine refractive index. *ChemPhysChem* **2018,** *19* (24), 3418-3424.
17. Hepp, K.; Lieb, E. H., On the superradiant phase transition for molecules in a quantized radiation field: the Dicke maser model. *Ann. Phys.* **1973,** *76* (2), 360-404.
18. Kavokin, A. V.; Baumberg, J. J.; Malpuech, G.; Laussy, F. P., *Microcavities*. Oxford university press: 2017; Vol. 21.
19. Hopfield, J., Theory of the contribution of excitons to the complex dielectric constant of crystals. *Physical Review* **1958,** *112* (5), 1555.
20. Doronin, I. V.; Kalmykov, A. S.; Zyablovsky, A. A.; Andrianov, E. S.; Khlebtsov, B. N.; Melentiev, P. N.; Balykin, V. I., Resonant concentration-driven control of dye molecule photodegradation via strong optical coupling to plasmonic nanopatricles. *Nano Lett.* **2022,** *22* (1), 105-110.
21. Thompson, R.; Rempe, G.; Kimble, H., Observation of normal-mode splitting for an atom in an optical cavity. *Physical review letters* **1992,** *68* (8), 1132.
22. Benson, R. C.; Kues, H. A., Absorption and fluorescence properties of cyanine dyes. *Journal of Chemical and Engineering Data* **1977,** *22* (4), 379-383.
23. Blaha, M.; Johnson, A.; Rauschenbeutel, A.; Volz, J., Beyond the Tavis-Cummings model: Revisiting cavity QED with ensembles of quantum emitters. *Physical Review A* **2022,** *105* (1), 013719.
24. López, C.; Christ, H.; Retamal, J.; Solano, E., Effective quantum dynamics of interacting systems with inhomogeneous coupling. *Physical Review A* **2007,** *75* (3), 033818.
25. Tserkezis, C.; Fernández-Domínguez, A. I.; Gonçalves, P.; Todisco, F.; Cox, J. D.; Busch, K.; Stenger, N.; Bozhevolnyi, S. I.; Mortensen, N. A.; Wolff, C., On the applicability of quantum-optical concepts in strong-coupling nanophotonics. *Reports on Progress in Physics* **2020,** *83* (8), 082401.
26. Koenderink, A. F., On the use of Purcell factors for plasmon antennas. *Optics letters* **2010,** *35* (24), 4208-4210.
27. Scully, M. O.; Zubairy, M. S., Quantum optics. American Association of Physics Teachers: 1999.
28. Nikoobakht, B.; El-Sayed, M. A., Preparation and growth mechanism of gold nanorods (NRs) using seed-mediated growth method. *Chemistry of Materials* **2003,** *15* (10), 1957-1962.